

Research Article

Production of Biologically Activated Carbon from Orange Peel and Landfill Leachate Subsequent Treatment Technology

Zhigang Xie, Wei Guan, Fangying Ji, Zhongrong Song, and Yanling Zhao

Chongqing Key Laboratory of Environmental Materials & Remediation Technologies,
Chongqing University of Arts and Sciences, Chongqing 402160, China

Correspondence should be addressed to Wei Guan; guanwei951030@126.com

Received 28 April 2014; Revised 20 May 2014; Accepted 20 May 2014; Published 23 June 2014

Academic Editor: Fan Dong

Copyright © 2014 Zhigang Xie et al. This is an open access article distributed under the Creative Commons Attribution License, which permits unrestricted use, distribution, and reproduction in any medium, provided the original work is properly cited.

In order to improve adsorption of macromolecular contaminants and promote the growth of microorganisms, active carbon for biological wastewater treatment or follow-up processing requires abundant mesopore and good biophile ability. In this experiment, biophile mesopore active carbon is produced in one-step activation with orange peel as raw material, and zinc chloride as activator, and the adsorption characteristics of orange peel active carbon is studied by static adsorption method. BET specific surface area and pore volume reached $1477 \text{ m}^2/\text{g}$ and $2.090 \text{ m}^3/\text{g}$, respectively. The surface functional groups were examined by Fourier transform infrared spectroscopy (FT-IR). The surface of the as-prepared activated carbon contained hydroxyl group, carbonyl group, and methoxy group. The analysis based on X-ray diffraction spectrogram (XRD) and three-dimensional fluorescence spectrum indicated that the as-prepared activated carbon, with smaller microcrystalline diameter and microcrystalline thickness and enhanced reactivity, exhibited enhanced adsorption performance. This research has a deep influence in effectively controlling water pollution, improving area water quality, easing orange peel waste pollution, and promoting coordinated development among society, economy, and environment.

1. Introduction

There is still no economic and applicable treatment method to deal with the wastewater after biochemical process with high residual concentration of COD and BOD [1–3]. Especially, the concentration of COD and $\text{NH}_3\text{-N}$ of landfill leachate reached 419~622 mg/L and 12.4~174.0 mg/L, respectively [4]. Moreover, BOD_5/COD is less than 0.012 [5]. This result leads to a serious imbalance ratio of C : N : P. Thus, the wastewater is difficult to be further biodegradation. In addition, the landfill leachate after biochemical treatment still contains a lot of naphthenic hydrocarbons, esters, carboxylic acids, phenol, and other toxic substances [6, 7]. Therefore, developing an efficient, stable, and advanced treatment of wastewater is of great technological and scientific significance.

Biological activated carbon (BAC) has great advantages in low concentration and refractory organic wastewater degradation [8–10]. The advantages of BAC include several aspects as follows. (1) The adsorption function of active carbon [11,

12]: organic matter is enriched in carbon particles, increasing contact time of organic matter and microorganisms and providing favorable conditions for microbial acclimation, so that the refractory material can be removed [13, 14]. (2) Adsorption of active carbon increases organic matter concentration around carbon particles, which is favorable to biological degradation [15, 16]. (3) The rough surface with cracks and honeycomb pits provides residential area for dominant bacteria to evade fluid shear stress [17, 18]. (4) The active carbon with strong adsorption capacity can absorb dissolved organic matters (DOMs). These DOMs provide food for the dominant bacteria [19, 20]. (5) Intense microbial activity accelerated the removal of organic matter. Even in the condition of low organic content, microorganisms still grow actively and decompose organic matter constantly due to the accumulation of carbon surface. And then the concentration of organics in the effluent decreased [21, 22]. (6) Active carbon reduces the effect of harmful substances to microorganism in water [23, 24]. This is mainly because the

adherent microorganism can resist poison of biodegradable organic compounds.

Orange peel with porous structure possesses hydrophilic surface group [25]. This is a cheap adsorbent. The adsorption can be enhanced by carbonization and activation [26]. During the activation process, activator can get into the interface due to the natural pore of orange peel [27]. Thus, the activation reaction can be in progress under a mild condition. The as-prepared active carbon with loose pore structure and large specific surface area and massive surface functional groups possesses favorable biophile characteristic and adsorption performance.

In this study, biophile mesopore active carbon was prepared by waste orange peel as raw material to deal with effluent of landfill leachate after biochemical treatment. Based on experiments, peel biological activated carbon technology for wastewater treatment was developed. Furthermore, a subsequent processing method for refractory organic leachate was investigated.

2. Materials and Methods

2.1. Raw Materials. The raw materials of producing active carbon are the processed orange pomace obtained from Chongqing Three Gorges Fruit Group. This citrus pericarp was dried and crushed sieving through 60-mesh sieve. The specifications and production units of reagents and materials used in this experiment are KBr, $ZnCl_2$, I_2 , KI, HCl, N_2 , and H_2O , respectively.

2.2. Preparation of Orange Peel Activated Carbon. Prior to the preparation experiment, orange peel was cleaned, cut, dried, and then crushed. 10 g samples were immersed into 100 mL zinc chloride solution. After 36 h, these samples were centrifuged from the solution and dried. And then, we added proper amount of coal tar and mixed with samples. The samples with partial size of 5~8 mm were formed by extrusion.

The heating process was under the protection of nitrogen. The flow of nitrogen was 0.2 mL/min. The reaction temperature increased to 150°C with 3°C/min, and the reaction time is 30 min when the temperature reached 150°C. Then, we increased the temperature to 300°C continuously to carbonize for 30 min. Solid samples were taken out when the temperature decreased to 20°C and were cleaned by 10% HCl and deionized water successively. The as-prepared citrus peel granular activated carbon was obtained after being dried at 105°C. The preparation process is shown in Figure 1.

The proper preparation condition of activated carbon is as follows: reaction temperature of 550°C; impregnation ratio of 3 : 1; and reaction time of 1 h.

2.3. Experimental Installation. Biological active carbon reactor (BAC) and process chart are shown in Figure 2. Biological active carbon pool was made of organic glass, which is a column reactor. The height of carbon pool is 2 m. Inside diameter is 63 mm. The filling height is 1800 mm. The carbon layer height is 1500 mm. The sand filters height is 300 mm.

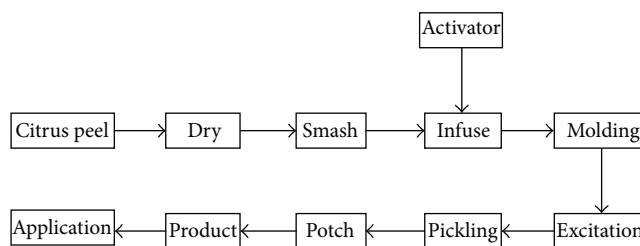


FIGURE 1: Preparing process of activated carbon from orange peel.

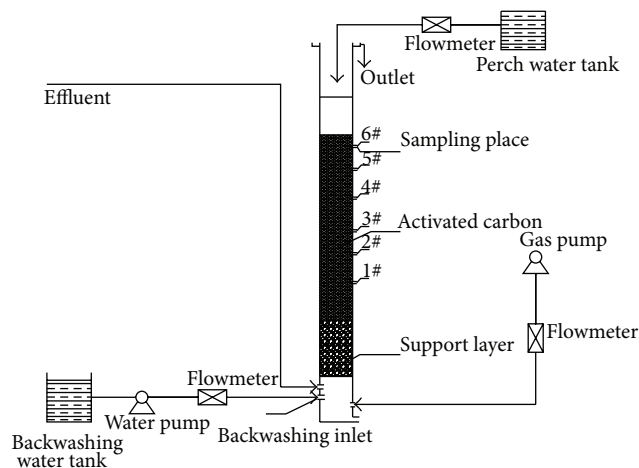


FIGURE 2: Biological activated carbon reactor.

The effective reaction volume is 4.7 L. There are 5 water sampling ports along with carbon pool. And there are aerators in the bottom and overflow weir in the top of carbon pool. The indicator of water quality analysis is UV_{254} (ultraviolet spectrophotometry and ultraviolet spectrophotometer).

2.4. Characterization Instruments. The crystal phases of the sample were analyzed by X-ray diffraction using $Cu K\alpha$ radiation (XRD, model XD-2 instrument, Persee, China). Nitrogen adsorption-desorption isotherms were obtained on a nitrogen adsorption apparatus (ASAP-2010, USA). All the samples were degassed at 200°C prior to measurements. Fourier transformed infrared spectroscopy (FT-IR, IR Prestige-21FT-infrared spectrometer, Shimadzu, Japan) was measured on FT-IR spectrometer on the transmission mode in the KBr pellet technique: resolution is 4 cm^{-1} and scan is 40 times. The morphology was observed by transmission electron microscope (TEM, JEOL JEM-2010, Japan). 3DEEM of examined water was obtained by F-7000 fluorescence spectrophotometer (Hitachi, USA).

3. Results and Discussion

3.1. FT-IR Analysis. The orange peel mesoporous active carbon and commercial active carbon were analyzed by FT-IR spectra (Figure 3). As shown in Figure 3, orange peel shows 4 strong absorption peaks in the region of $3500\sim 1000\text{ cm}^{-1}$.

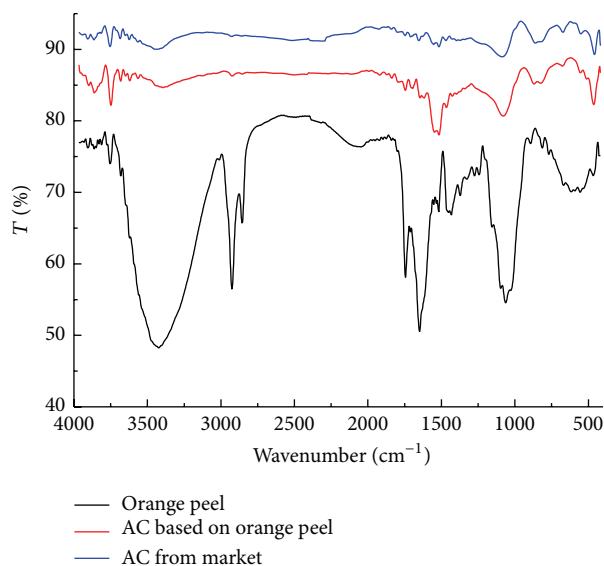


FIGURE 3: FT-IR spectrum of orange peel and activated carbon samples.

These peaks could be attributed to the antisymmetric stretching vibration of -OH (at 3435.07 cm^{-1}), -CH_3 and -CH_2 (at 2924.31 cm^{-1}), and C=O (at 1646.40 cm^{-1}), respectively [28]. The peak at 1068.77 cm^{-1} was attributed to the vibration absorption of C-O . These peaks indicated that the orange peel contains a lot of cellulose and hemicelluloses. After being carbonized, the absorption peaks at $3500\sim 1700\text{ cm}^{-1}$ disappeared. This indicated that the crystal structure of cellulose molecular chain has been destructed.

After being carbonized, the as-prepared mesoporous active carbon and commercial active carbon show the stretch vibration absorption spectra of -OH at 3750 cm^{-1} and 3420 cm^{-1} . The peak at 1840 cm^{-1} belongs to the nonsymmetric vibration absorption of C=O , and peak at $1750\sim 1640\text{ cm}^{-1}$ is the stretching vibration absorption of C=O . This indicated that the mesoporous active carbon and commercial carbon contain hydroxyl, carbonyl products, methoxy, and lactones. In comparison, the adsorption peak of mesoporous active carbon is stronger than the other. Strong absorption peak of mesoporous active carbon in $1630\sim 1520\text{ cm}^{-1}$ is stretching vibration of benzene ring skeleton. In addition, there is a C-H symmetric stretching vibration peak at 2820 cm^{-1} . The adsorption peak of commercial carbon at $1630\sim 1520\text{ cm}^{-1}$ is weak, indicating the mesoporous active carbon containing more orange. Natural groups of citrus peel active carbon were retained to hydrophilic groups, which have strong biophile characteristics.

3.2. Microstructure of Citrus Peel Active Carbon. The microstructure of citrus peel active carbon was observed using TEM (Figure 4). TEM shows that citrus peel active carbon has rich mesoporous with a few large pores. The developed pore structure of active carbon is useful for attachment of microorganisms.

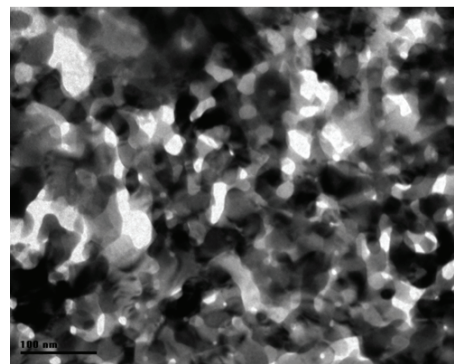


FIGURE 4: TEM image of orange peel activated carbon.

3.3. The Pore Size Distribution of Citrus Peel Active Carbon.

Figure 5 shows N_2 adsorption-desorption isotherms and pore-size distribution curves of citrus peel mesoporous active carbon and commercial active carbon. As seen in Figure 5, according to analyzing adsorption characteristics of activated carbon from the orange peel, it was found that it had the characteristics of type I adsorption isotherm. The specific surface area of biological activated carbon and commercial activated carbon is $1477\text{ m}^2/\text{g}$ and $977\text{ m}^2/\text{g}$, respectively. The pore structure of orange peel active carbon is mesoporous with $2.0\text{ nm}\sim 4.0\text{ nm}$. Mesoporosity reached 68.9%. The average pore size of citrus peel active carbon is $2.0\sim 4.0\text{ nm}$. This pore structure is beneficial to microbial nutrient matrix and the growth of the microorganisms.

3.4. The XRD Analysis of Citrus Peel Active Carbon.

Figure 6 is the XRD patterns of citrus peel active carbon and commercial active carbon. As shown in Figure 6, the strong and weak diffraction peaks emerged at $2\theta = 25^\circ$ and $2\theta = 45^\circ$, respectively. This result indicates the existence of graphite crystallite in citrus peel active carbon and commercial active carbon. The diffraction peaks of commercial active carbon are sharper than those of citrus peel active carbon, indicating that crystallite size of citrus peel active carbon is smaller. This result can be proven by the data of Table 1.

The whole wall of activated carbon is composed of graphite crystallite scale decreases, which can lead to widening or internal structure disordered, so as to form a larger specific surface area. The activated carbon is comprised of ultrafine particles possesses porous structure. The lower the crystallinity, the larger the specific surface area.

There is a close relationship between the degree of graphitization and the interplanar spacing D_{002} of carbon materials. The smaller the value of carbon crystallites D_{002} is, the higher the degree of graphitization might be. As shown in Figure 6, compared with commercial activated carbon, the diffraction angle of citrus peels active carbon decreased, indicating that the degree of graphitization of citrus peels active carbon is higher than that of commercial active carbon. The decrease of microcrystalline strength leads to the stronger activity of active carbon. This result indicates that the orange peel active carbon substratum graphite trend is obvious.

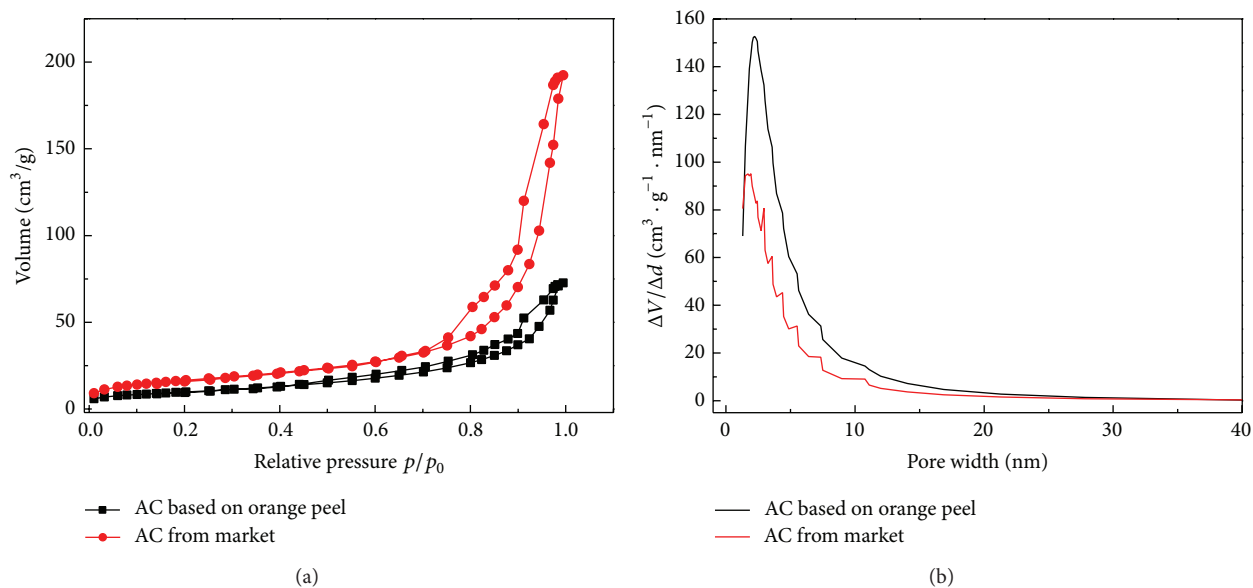


FIGURE 5: N_2 adsorption-desorption isotherms (a) and pore-size distribution curves (b) of citrus peel mesoporous active carbon and commercial active carbon.

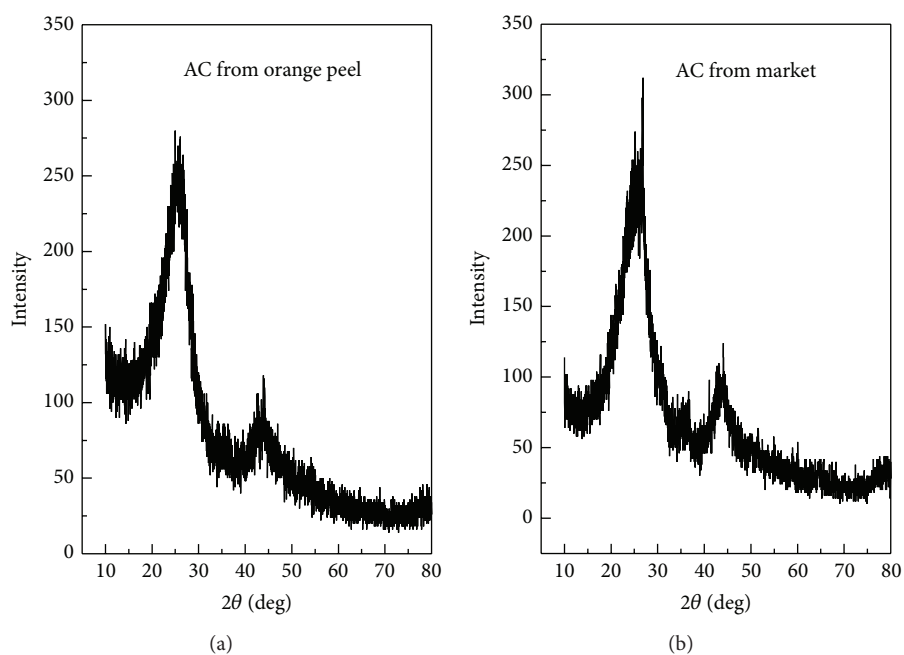


FIGURE 6: XRD pattern of activated carbon.

TABLE 1: Crystalline parameters of activated carbon.

Samples	Microcrystalline diameter L_a/nm	Microcrystalline thickness L_c/nm	d_{002}/nm	d_{100}/nm
Orange peel Active Carbon	2.7831	0.7541	0.3485	0.2059
Commercial Active Carbon	3.7914	0.9832	0.3331	0.2153

TABLE 2: The main performance parameters of activated carbon in experiment.

Index	Orange peel active carbon	Commercial active carbon
Grain size/mm	3.0	2.0
Specific surface area/(m ² /g)	1477	960
Average pore size/mm	3.87	2.02
Micropore volume/(cm ³ /g)	0.532	0.201
Mesopore volume/(cm ³ /g)	1.440	0.616
Total pore volume/(cm ³ /g)	2.090	0.900

3.5. *Adsorption Properties of Orange Peel Active Carbon.* Table 2 is the structure parameters of orange peel active carbon and commercial active carbon. Figure 7 is the static adsorption curve of orange peel active carbon and commercial active carbon. Dosage of active carbon is 0.2 g, and the volume of biochemical water is 50 mL. Figure 8 is the TEM photographs of orange peel active carbon after absorbing biochemical water. Figure 9 is 3DEEM of biochemical water before and after being absorbed by orange peel active carbon.

According to Figure 7, orange peel active carbon exhibited good properties to adsorb biochemical water. The concentration of UV₂₅₄ and TOC has a similar change trend. The removal efficiency of UV₂₅₄ and TOC is 63.0% and 59.7%, respectively. The adsorption property of commercial active carbon is weak. The removal efficiency of UV₂₅₄ and TOC is only 52.9% and 24.8%. According to Table 2, the pore volume of commercial active carbon is smaller than that of orange peel active carbon. There were two stages in the UV₂₅₄ removal curves by citrus peel AC in Figure 7; they corresponded to the film diffusion and particle diffusion, respectively.

According to the TEM photographs in Figure 8, the pore structure of orange peel active carbon filled with the amount of organic matter, which means that the pores of active carbon can effectively absorb pollutants in leachate tail water.

As seen in Figure 9, biochemical leachate tail water DOM has two obvious fluorescence peaks: UV fulvic-like fluorescence (Ex/Em = 255/455 nm, Peak, A) and visible fulvic-like fluorescence (Ex/Em = 330/405 nm, Peak, C), containing carboxyl and carbonyl groups. After being adsorbed by orange peel active carbon, ultraviolet water fulvic-like fluorescence intensity (IA) drops from 2222 to 1132, reduced by 49.1%. Visible fulvic-like fluorescence intensity (IC) drops from 1840 to 338.8, reduced by 81.6%. Ex of peak A shift to 250 nm after adsorption. The blue shift of absorption bands for Ex and Em of peak C was observed (Ex/Em = 315/400 nm), and the fluorescence peak center disappears and only the long band exists. This shows that orange peel active carbon has good adsorption properties for water class fulvic acids and other organic matters.

3.6. *Adsorption Kinetics of Citrus Peel Active Carbon.* Based on adsorption kinetics, the adsorption law of orange peel

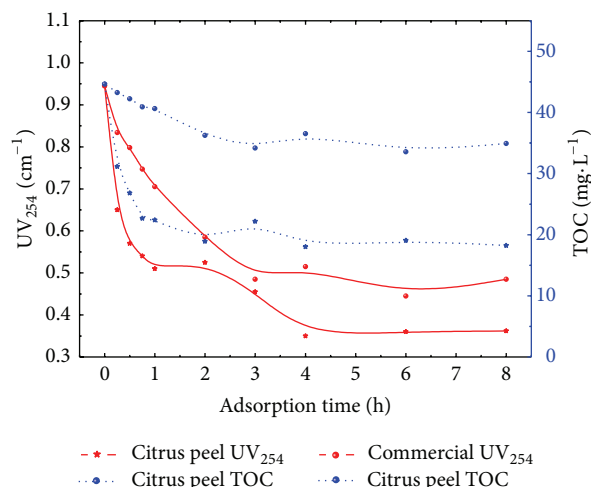


FIGURE 7: Adsorption property of activated carbon.

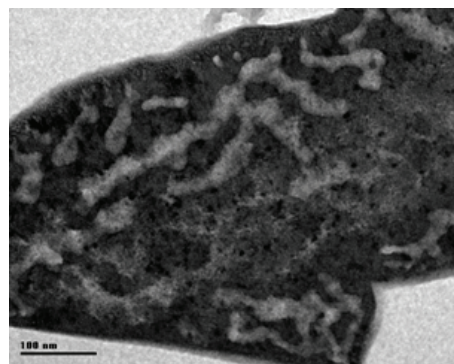


FIGURE 8: TEM image of activated carbon from orange peel after adsorbing organic matters.

active carbon was studied at 25°C, 35°C, and 45°C, respectively. The absorptivity of active carbon can be calculated by

$$q = V \times \frac{(c_0 - c)}{(1000m)}, \quad (1)$$

where q is adsorption, mg/g, V is adsorbed solution volume, mL, c_0 and c are the concentration of TOC in water, respectively, mg/L, and m is the quality of active carbon.

According to Figure 10, under different temperature conditions, the absorbance of TOC increased quickly in the initial 1h and reached adsorption equilibrium after 4h. The absorbance decreased with the increase of temperature. This indicates that lower temperature is beneficial to the adsorption process of active carbon.

The Lagergren equation (pseudo-first-order kinetic equation) adsorption mechanism and pseudo-two-order kinetics equation are suitable for the expression of the solid adsorption mechanism in aqueous solution [29]. Lagergren kinetic equation can be expressed as follows:

$$\frac{dq}{dt} = k_1 (q_e - q), \quad (2)$$

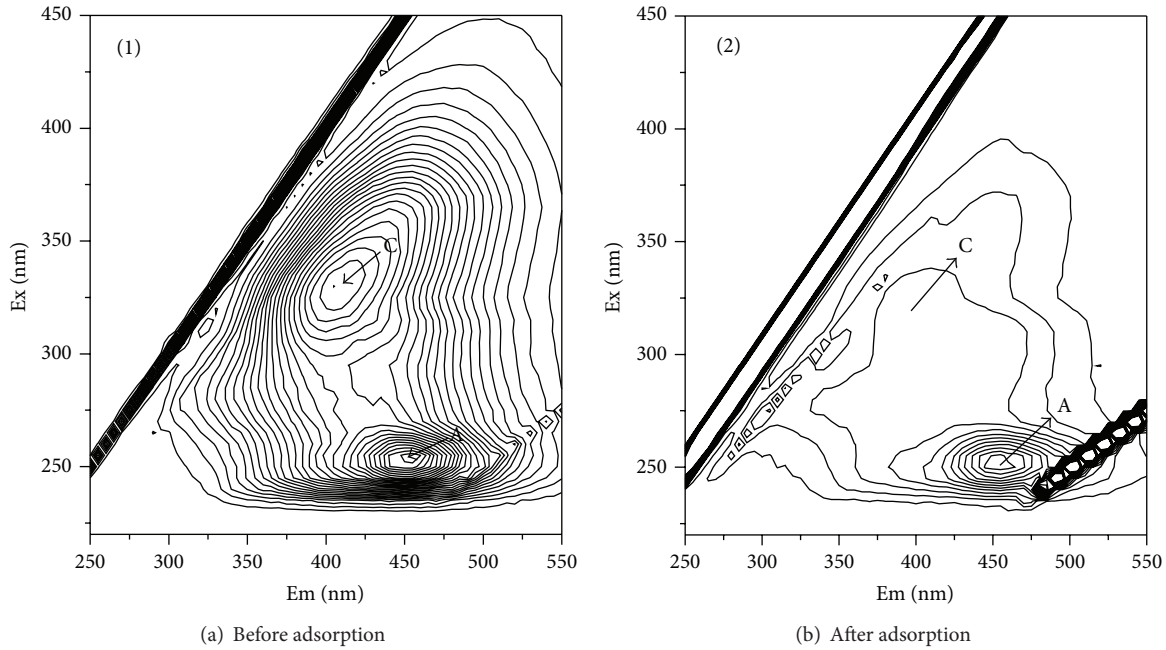


FIGURE 9: 3DEEM for dissolved organic matters of leachate biochemical treatment effluent.

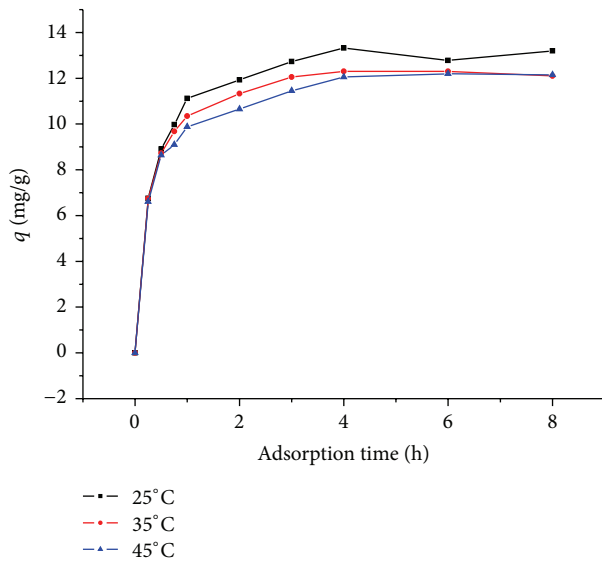


FIGURE 10: Effect of contact time on TOC adsorption of activated carbon.

where q_e is the equilibrium adsorption capacity (mg/g); q is adsorption quantity at a time (mg/g); and k_1 is adsorption kinetics rate constant (min^{-1}). Equation (1) can be integral as follows:

$$\lg(q_e - q) = \lg q_e - \frac{k_1 t}{2.303}. \quad (3)$$

The pseudo-second-order model provided by Ho has been widely used to describe the various adsorption systems. The pseudo-second-order model can be expressed as

$$\frac{dq}{dt} = k_1(q_e - q)^2, \quad (4)$$

where k is the adsorption rate constant [$\text{g}(\text{mg} \cdot \text{h})^{-1}$]. The integral linear can be expressed as follows:

$$\frac{t}{q} = \frac{1}{k_2 q_e^2} + \frac{t}{q_e}. \quad (5)$$

Intraparticle diffusion model can be expressed as follows:

$$q_t = k_p t^{0.5}, \quad (6)$$

where k_p is the diffusion rate constant [$\text{mg}/(\text{g} \cdot \text{min})$].

Liquid film diffusion model can be expressed as follows:

$$\ln\left(\frac{c_t}{c_0}\right) = \frac{-k_f A t}{V}, \quad (7)$$

where c_0 , c_t , A/V , and t are the initial concentration, the concentration at t min, the adsorption area, the ratio of volume of solution, and adsorption time, respectively, and k_f is the diffusion coefficient.

The experiment data of the adsorption process can be fitted by (3) and (4), respectively (Figures 11(a) and 11(b)). According to Figures 11(a) and 11(b), the adsorption data of citrus peel activated carbon on TOC can be fitted by Lagergren kinetic equation (proposed a kinetic equation) and proposed two kinetic equations. The correlation coefficient

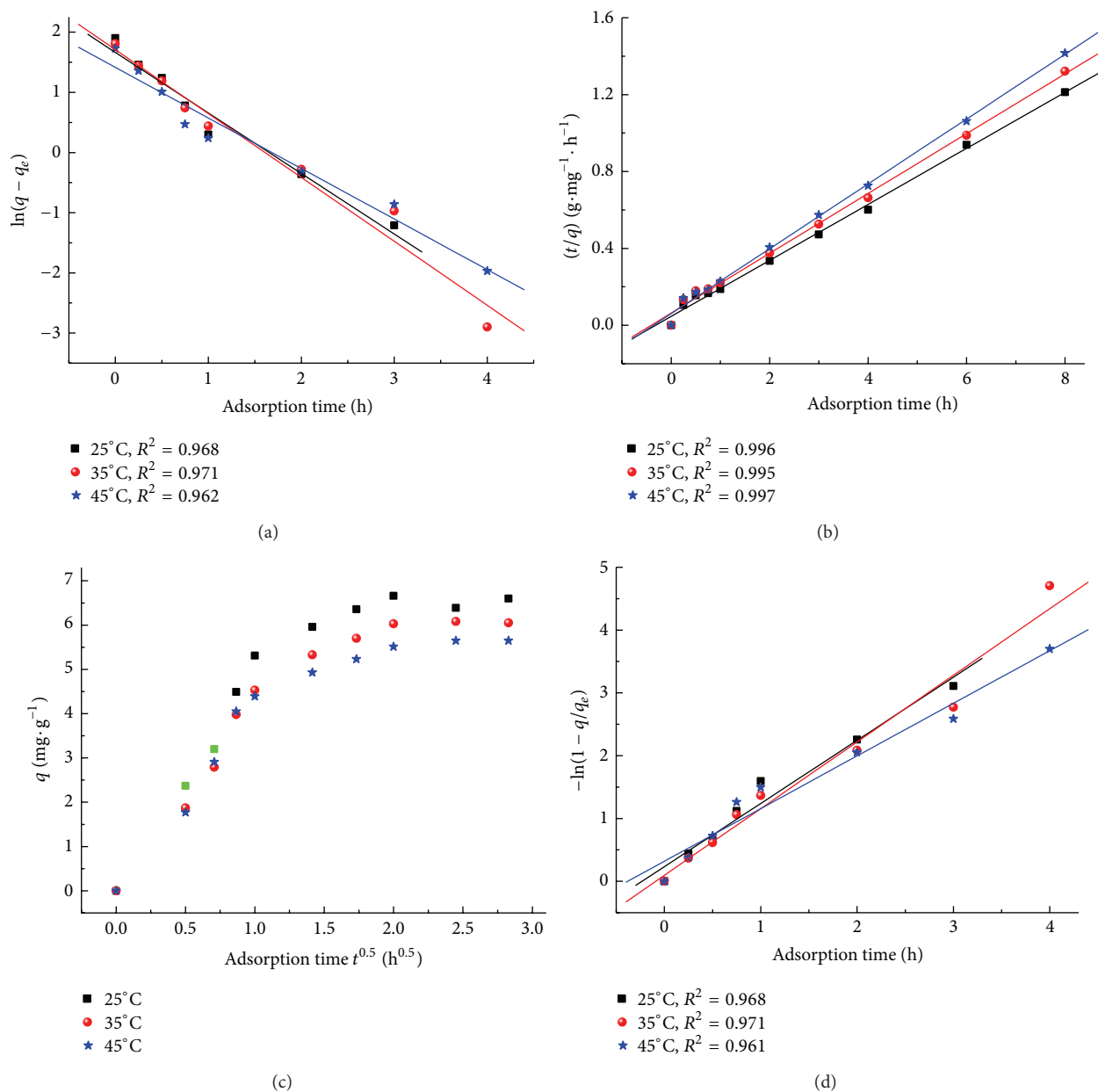


FIGURE 11: Adsorption kinetics models of activated carbon, (a) Lagergren model, (b) pseudo-second-order model, (c) intraparticle diffusion model, and (d) liquid film diffusion model.

R^2 of Lagergren kinetic equation is 0.961~0.969, and the correlation coefficient R^2 of proposed two kinetic equations is 0.961~0.969. Higher correlation coefficient indicating the second-order equation is proper to describe the adsorption mechanism of active carbon to deal with biochemical leachate tail water.

The diffusion rate of absorbent in the interface of active carbon increased with the increasing temperature. Thus, the adsorption rate constant increased with the increasing adsorption rate. The adsorption process of active carbon includes three steps, such as film diffusion, the particle diffusion, and adsorption reaction. Adsorption reaction is the

fast step. The plot q to $t^{0.5}$ in Figure 11(c) and the plot $\ln(1 - q/q_e)$ to t are shown in Figure 11(d). According to Figure 11(c), there is an inflection point between 1.0~1.5 h, indicating that the influencing factors include particle internal diffusion and liquid membrane diffusion. As seen in Figure 11(d), there is a straight line deviating from the origin, indicating that film diffusion is the main rate control step in the early adsorption. The absorbate can be absorbed only through the film arriving carbon surface. Organic molecules through the film are a few in the early adsorption and can be absorbed in carbon surface quickly. Therefore, film diffusion is rate control step. When organic molecules arrived, carbon surface increased

to a certain extent; the particle diffusion is adsorption rate control step.

4. Conclusion

Based on the analysis of characteristics of orange peel, this study provides an innovative idea that the natural pore structure of orange peel is beneficial for the formation of mesoporous active carbon. In this paper, orange peel activated carbon with biophile characteristic has been prepared by one-step method. The yield of the as-prepared biological activated carbon is 50.9%. Orange peel active carbon has hydroxyl, carbonyl, methoxy, and lactones hydrophilic functional group. XRD analysis indicates that the substratum trend of orange peel active carbon is obvious. The orange peel active carbon exhibited enhanced reactivity due to small crystallite size and crystallite thickness. The static adsorption experiment indicated that orange peel active carbon has a good adsorption to deal with leachate biochemical tail water. The removal rate of UV_{254} is 63.0% and TOC is 59.7%, respectively. Three-dimensional fluorescence spectroscopy has been used to follow the adsorption process. Orange peel active carbon exhibited enhanced ability to adsorb fulvic acids in leachate biochemical water. This research has a deep positive influence in effectively controlling water pollution, improving area water quality, easing orange peel waste pollution, and promoting coordinated development among society, economy, and environment.

Conflict of Interests

The authors declare that they have no conflict of interests regarding the publication of this paper.

Acknowledgments

This work was supported by the Municipal Education Commission Funded Project of Chongqing, China (KJ111203), and the Construction Science and Technology Project of Chongqing (2011-2-115).

References

- [1] D. A. Jones, T. P. Lelyveld, S. D. Mavrofidis, S. W. Kingman, and N. J. Miles, "Microwave heating applications in environmental engineering—a review," *Resources, Conservation and Recycling*, vol. 34, no. 2, pp. 75–90, 2002.
- [2] F. R. Kolb and P. A. Wilder, "Activated carbon adsorption couple with biodegradation to treat problematic wastewater," in *Proceedings of the 1st IAWQ Specialized Conference on Adsorption in Water Environment and Treatment Process*, pp. 191–199, Wadayama, Japan, 1996.
- [3] K. Mochidzuki and Y. Takeuchi, "The effects of some inhibitory components on biological activated carbon processes," *Water Research*, vol. 33, no. 11, pp. 2609–2616, 1999.
- [4] M. Cháfer, C. González-Martínez, A. Chiralt, and P. Fito, "Microstructure and vacuum impregnation response of citrus peels," *Food Research International*, vol. 36, no. 1, pp. 35–41, 2003.
- [5] K. N. Ghimire, K. Inoue, H. Yamaguchi, K. Makino, and T. Miyajima, "Adsorptive separation of arsenate and arsenite anions from aqueous medium by using orange waste," *Water Research*, vol. 37, no. 20, pp. 4945–4953, 2003.
- [6] M. Ajmal, R. A. K. Rao, R. Ahmad, and J. Ahmad, "Adsorption studies on Citrus reticulata (fruit peel of orange): removal and recovery of Ni(II) from electroplating wastewater," *Journal of Hazardous Materials*, vol. 79, no. 1-2, pp. 117–131, 2000.
- [7] A. B. Pérez-Marín, V. M. Zapata, J. F. Ortuño, M. Aguilar, J. Sáez, and M. Lloréns, "Removal of cadmium from aqueous solutions by adsorption onto orange waste," *Journal of Hazardous Materials*, vol. 139, no. 1, pp. 122–131, 2007.
- [8] Z. Xuan, Y. Tang, X. Li, Y. Liu, and F. Luo, "Study on the equilibrium, kinetics and isotherm of biosorption of lead ions onto pretreated chemically modified orange peel," *Biochemical Engineering Journal*, vol. 31, no. 2, pp. 160–164, 2006.
- [9] C. Namasivayam, N. Muniasamy, K. Gayatri, M. Rani, and K. Ranganathan, "Removal of dyes from aqueous solutions by cellulosic waste orange peel," *Bioresource Technology*, vol. 57, no. 1, pp. 37–43, 1996.
- [10] R. Sivaraj, C. Namasivayam, and K. Kadirvelu, "Orange peel as an adsorbent in the removal of Acid violet 17 (acid dye) from aqueous solutions," *Waste Management*, vol. 21, no. 1, pp. 105–110, 2001.
- [11] K. V. Kumar and K. Porkodi, "Batch adsorber design for different solution volume/adsorbent mass ratios using the experimental equilibrium data with fixed solution volume/adsorbent mass ratio of malachite green onto orange peel," *Dyes and Pigments*, vol. 74, no. 3, pp. 590–594, 2007.
- [12] M. Arami, N. Y. Limaee, N. M. Mahmoodi, and N. S. Tabrizi, "Removal of dyes from colored textile wastewater by orange peel adsorbent: Equilibrium and kinetic studies," *Journal of Colloid and Interface Science*, vol. 288, no. 2, pp. 371–376, 2005.
- [13] G. Annadurai, R. S. Juang, and D. J. Lee, "Use of cellulose-based wastes for adsorption of dyes from aqueous solutions," *Journal of Hazardous Materials*, vol. 92, no. 3, pp. 263–274, 2002.
- [14] B. Ozkaya, "Chlorophenols in leachates originating from different landfills and aerobic composting plants," *Journal of Hazardous Materials*, vol. 124, no. 1-3, pp. 107–112, 2005.
- [15] P. J. He, L. M. Shao, X. Qu, G. J. Li, and D. J. Lee, "Effects of feed solutions on refuse hydrolysis and landfill leachate characteristics," *Chemosphere*, vol. 59, no. 6, pp. 837–844, 2005.
- [16] R. J. Slack, J. R. Gronow, and N. Voulvoulis, "Household hazardous waste in municipal landfills: contaminants in leachate," *Science of the Total Environment*, vol. 337, no. 1-3, pp. 119–137, 2005.
- [17] A. A. Bakare, A. A. Mosuro, and O. Osibanjo, "An in vivo evaluation of induction of abnormal sperm morphology in mice by landfill leachates," *Mutation Research*, vol. 582, no. 1-2, pp. 28–34, 2005.
- [18] L. N. Huang, S. Zhu, H. Zhou, and L. H. Qu, "Molecular phylogenetic diversity of bacteria associated with the leachate of a closed municipal solid waste landfill," *FEMS Microbiology Letters*, vol. 242, no. 2, pp. 297–303, 2005.
- [19] N. Sang and G. Li, "Chromosomal aberrations induced in mouse bone marrow cells by municipal landfill leachate," *Environmental Toxicology and Pharmacology*, vol. 20, no. 1, pp. 219–224, 2005.
- [20] G. Gupta and W. Gardner, "Use of clay mineral (montmorillonite) for reducing poultry litter leachate toxicity (EC50)," *Journal of Hazardous Materials*, vol. 118, no. 1-3, pp. 81–83, 2005.

- [21] C. Visvanathan, M. K. Choudhary, M. T. Montalbo, and V. Jegatheesan, "Landfill leachate treatment using thermophilic membrane bioreactor," *Desalination*, vol. 204, no. 1–3, pp. 8–16, 2007.
- [22] E. Noaksson, M. Linderöth, B. Gustavsson, Y. Zebühr, and L. Balk, "Reproductive status in female perch (*Perca fluviatilis*) outside a sewage treatment plant processing leachate from a refuse dump," *Science of the Total Environment*, vol. 340, no. 1–3, pp. 97–112, 2005.
- [23] H. D. Robinson, K. Knox, B. D. Bone, and A. Picken, "Leachate quality from landfilled MBT waste," *Waste Management*, vol. 25, no. 4, pp. 383–391, 2005.
- [24] M. Mavros, N. P. Xekoukoulotakis, D. Mantzavinos, and E. Diamadopoulos, "Complete treatment of olive pomace leachate by coagulation, activated-carbon adsorption and electrochemical oxidation," *Water Research*, vol. 42, no. 12, pp. 2883–2888, 2008.
- [25] M. C. Mittelmeijer-Hazeleger and J. M. Martín-Martínez, "Microporosity development by CO₂ activation of an anthracite studied by physical adsorption of gases, mercury porosimetry, and scanning electron microscopy," *Carbon*, vol. 30, no. 4, pp. 695–709, 1992.
- [26] K. Tomków, T. Siemienińska, F. Czechowski, and A. Jankowska, "Formation of porous structures in activated brown-coal chars using O₂, CO₂ and H₂O as activating agents," *Fuel*, vol. 56, no. 2, pp. 121–124, 1977.
- [27] M. Jagtoyen, M. Thwaites, J. Stencil, B. McEnaney, and F. Derbyshire, "Adsorbent carbon synthesis from coals by phosphoric acid activation," *Carbon*, vol. 30, no. 7, pp. 1089–1096, 1992.
- [28] W. Jiang, J. A. Joens, D. D. Dionysiou, and K. E. O'Shea, "Optimization of photocatalytic performance of TiO₂ coated glass microspheres using response surface methodology and the application for degradation of dimethyl phthalate," *Journal of Photochemistry and Photobiology A: Chemistry*, vol. 262, pp. 7–13, 2013.
- [29] B. S. Girgis, L. B. Khalil, and T. A. M. Tawfik, "Activated carbon from sugar cane bagasse by carbonization in the presence of inorganic acids," *Journal of Chemical Technology and Biotechnology*, vol. 61, no. 1, pp. 87–92, 1994.



Hindawi

Submit your manuscripts at
<http://www.hindawi.com>

